Research Article | Vol. 25, No. 3 | 6 Feb 2017 | OPTICS EXPRESS 2939

Optics EXPRESS

Passive photonic integrated ratiometric wavelength monitor with resolution better than 15 pm

PENGFEI WANG,[1,2,*] AGUS MUHAMAD HATTA,[3] HAOYU ZHAO,[1] WENLEI YANG,[1] JING REN,[1] YAXIAN FAN,[1] GERALD FARRELL,[2] AND GILBERTO BRAMBILLA[4]

[1]*Key Laboratory of In-fiber Integrated Optics of Ministry of Education, College of Science, Harbin Engineering University, Harbin 150001, China*
[2]*Photonic Research Centre, Dublin Institute of Technology, Kevin Street, Dublin 8, Ireland*
[3]*Department of Engineering Physics, Faculty of Industrial Technology, Institut Teknologi Sepuluh Nopember, Surabaya, Indonesia*
[4]*Optoelectronics Research Centre, University of Southampton, Southampton SO17 1BJ, United Kingdom*
**pengfei.wang@dit.ie*

Abstract: This paper presents a compact and low-loss photonic integrated device consisting of a Y-branch and a pair of multimode interferometers (MMI) for a ratiometric wavelength monitoring around 1550 nm on silicon-on-insulator (SOI) technique. Two MMIs are designed in terms of width and length to achieve overlapping but opposite slope spectral responses used as two edge filters over a wavelength measurement range from 1500 nm to 1600 nm. The developed integrated photonic ratiometric structure demonstrates a suitable discrimination range for a high-speed passive wavelength measurement, with a high resolution better than 15 pm over a 100 nm wavelength range.

OCIS codes: (130.0130) Integrated optics; (130.3120) Integrated optics devices; (230.7370) Waveguides.

References and links

1. H. Nasu, T. Mukaihara, T. Takagi, M. Oike, T. Nomura, and A. Kasukawa, "25-GHz-spacing wavelength-monitor integrated DFB laser module for DWDM applications," IEEE Photonics Technol. Lett. **15**(2), 293–295 (2003).
2. Y. Sano and T. Yoshino, "Fast optical wavelength interrogator employing arrayed waveguide grating for distributed fiber Bragg grating sensors," J. Lightwave Technol. **21**(1), 132–139 (2003).
3. Q. Wang, G. Farrell, T. Freir, G. Rajan, and P. Wang, "Low-cost wavelength measurement based on a macrobending single-mode fiber," Opt. Lett. **31**(12), 1785–1787 (2006).
4. A. M. Hatta, G. Farrell, Q. Wang, G. Rajan, P. Wang, and Y. Semenova, "Ratiometric wavelength monitor based on singlemode-multimode-singlemode fiber structure," Microw. Opt. Technol. Lett. **50**(12), 3036–3039 (2008).
5. A. M. Hatta, G. Rajan, G. Farrell, and Y. Semenova, "Ratiometric wavelength monitor based on X-type spectral response using two edge filters," Proc. SPIE **7356**, 73561N (2009).
6. T. Allos, J. Bingham, R. Birss, and M. Parker, "Novel low-cost ratiometric photometer," J. Phys. E Sci. Instrum. **11**(12), 1195–1199 (1978).
7. Q. Wang, G. Farrell, P. Wang, G. Rajan, and T. Freir, "Design of integrated wavelength monitor based on a Y-branch with an S-bend waveguide," Sens. Actuators A Phys. **134**(2), 405–409 (2007).
8. G. Wang, A. Shen, C. Zhao, L. Yang, T. Dai, Y. Wang, Y. Li, X. Jiang, and J. Yang, "Fano-resonance-based ultra-high-resolution ratio-metric wavelength monitor on silicon," Opt. Lett. **41**(3), 544–547 (2016).
9. R. Soref, "The past, present, and future of silicon photonics," IEEE J. Sel. Top. Quantum Electron. **12**(6), 1678–1687 (2006).
10. R. Soref, "Mid-infrared photonics in silicon and germanium," Nat. Photonics **4**(8), 495–497 (2010).
11. Q. Wang and G. Farrell, "All-fiber multimode-interference-based refractometer sensor: proposal and design," Opt. Lett. **31**(3), 317–319 (2006).
12. Y. Zhang, Z. Li, and B. Li, "Multimode interference effect and self-imaging principle in two-dimensional silicon photonic crystal waveguides for terahertz waves," Opt. Express **14**(7), 2679–2689 (2006).
13. Y. Shi, D. Dai, and S. He, "Proposal for an ultracompact polarization-beam splitter based on a photonic-crystal-assisted multimode interference coupler," IEEE Photonics Technol. Lett. **19**(11), 825–827 (2007).

#282248 https://doi.org/10.1364/OE.25.002939
Journal © 2017 Received 22 Dec 2016; revised 20 Jan 2017; accepted 27 Jan 2017; published 3 Feb 2017

Optics EXPRESS

14. A. M. Hatta, G. Farrell, Y. Semenova, and H. Fernando, "Ratiometric wavelength monitor using a pair of symmetrical multimode interference structures based on silicon-on-insulator (SOI)," Proc. SPIE **7366**, 73660S (2009).
15. P. Wang, A. M. Hatta, H. Zhao, J. Zheng, G. Farrell, and G. Brambilla, "A ratiometric wavelength measurement based on a silicon-on-insulator directional coupler integrated device," Sensors (Basel) **15**(9), 21280–21293 (2015).
16. Q. Wang, J. Lu, and S. He, "Optimal design method of a low-loss broadband Y branch with a multimode waveguide section," Appl. Opt. **41**(36), 7644–7649 (2002).
17. L. B. Soldano, F. B. Veerman, M. K. Smit, B. H. Verbeek, A. H. Dubost, and E. Pennings, "Planar monomode optical couplers based on multimode interference effects," J. Lightwave Technol. **10**(12), 1843–1850 (1992).
18. M. Stern, "Semivectorial polarised finite difference method for optical waveguides with arbitrary index profiles," IEE Proc., Optoelectron. **135**(1), 56–63 (1988).
19. P. Wang, G. Farrell, Q. Wang, and G. Rajan, "An optimized macrobending-fiber-based edge filter," IEEE Photonics Technol. Lett. **19**(15), 1136–1138 (2007).
20. L. B. Soldano, F. B. Veerman, M. K. Smit, B. H. Verbeek, A. H. Dubost, and E. C. Pennings, "Planar monomode optical couplers based on multimode interference effects," J. Lightwave Technol. **10**(12), 1843–1850 (1992).
21. R. A. Soref, J. Schmidtchen, and K. Petermann, "Large single-mode rib waveguides in GeSi-Si and Si-on-SiO_2," IEEE J. Sel. Top. Quantum Electron. **27**(8), 1971–1974 (1991).
22. P. Wang, G. Farrell, and Y. Semenova, "Generalized design process for fiber-bend-loss-based edge filters for a wavelength measurement system," Appl. Opt. **48**(16), 3055–3061 (2009).
23. Q. Wang, G. Rajan, P. Wang, and G. Farrell, "Resolution investigation of a ratiometric wavelength measurement system," Appl. Opt. **46**(25), 6362–6367 (2007).

1. Introduction

Wavelength monitoring is exploited in many optical systems, such as dense wavelength division multiplexing (DWDM) and fiber Bragg gratings (FBGs) optical sensors [1,2], where an accurate measurement of wavelength is highly beneficial. There are numerous wavelength-monitoring schemes and among them the simplest way to monitor a wavelength change is to use a wavelength dependent optical filter with a linear response, which works by translating a wavelength change into an intensity change, assuming a suitable calibration has taken place. This method is based on the use of an edge filter, which has a linear response with a steep slope over a narrow range, or a broad band filter, which has a mild slope over a wide range. An edge filter based ratiometric measurement scheme [3], which utilizes the transition region of the filter spectral transmission response and undertakes wavelength monitoring by means of a signal-intensity measurement, has a simple configuration and offers the potential for high-speed measurements as compared with a number of active methods such as wavelength scanning based active measurement schemes.

Fiber optic sensing systems based on Fiber Bragg Gratings (FBGs) require a wavelength monitoring system to demodulate the wavelength shift induced by environmental changes on the light reflected from the FBG. A recent investigation has proven that wavelength monitoring can be implemented using a ratiometric power measurement technique [4]. A ratiometric wavelength monitor usually can be divided into two parts: a splitter and one/two edge filters. The splitter usually has two output ports one of which is used as a reference arm and the other is connected to an edge filter arm with a well-defined spectral response. Alternatively, both outputs can be connected to edge filters with overlapping opposite slope spectral responses [5], the so-called "X-type spectral response", to increase the resolution of the measurement system. The ratiometric scheme can be implemented by using a range of photonic components, such as a bulk device [6], an all-fiber based configuration [3] or an integrated optics device [7, 8].

The integrated wavelength monitor has the advantages of a compact size, a high scalability, and also benefits from low-cost and physical robustness compared to bulk devices and photonic devices based on all-fiber configurations.

Silicon photonics [9] enables both electronics and optics to be integrated on the same optoelectronic circuit chip, leading to the possible production of low-cost and simple configuration devices on a single silicon wafer by using standard microelectronic industrial processes. SOI is very attractive since it is one of the most promising platforms for achieving

Optics EXPRESS

dense integration of optoelectronic devices at low cost. Importantly, the main two materials of SOI wafers, the silicon and the oxide insulator (traditionally silica) are transparent at telecom wavelengths of λ = 1300 nm and 1550 nm, and in particular silicon has a low loss in the mid-infrared (IR) band [10]. Therefore an SOI based integrated photonic device has significant potential for applications in telecoms and possibly in the short wavelength region of the mid-IR.

Multimode interference (MMI) effects based photonic devices have been widely employed for a range of integrated photonics applications [11–13] because of their numerous unique advantages, such as compact physical structure, large operating bandwidth, relatively low insertion loss, ease of fabrication using photolithography and controllable manufacturing tolerance. Our previous investigation reported an all-fiber based ratiometric system which used two singlemode-multimode-singlemode (SMS) fiber structures based edge filters with an X-type spectral response [5]. In an effort to further miniaturize the all-fiber ratiometric wavelength monitor, a design of SOI MMI-based integrated ratiometric wavelength monitor was proposed [14]. In this paper, the wavelength monitor developed which includes one input waveguide, two MMI waveguides and two output waveguides is presented. The use of two symmetrical MMIs based on SOI provide a 100 nm range and a high resolution better than 15 pm, much better than that of 50 pm [15] previously reported.

2. Device structure design

The schematic configuration of the proposed photonic SOI integrated ratiometric wavelength monitoring system based on MMIs is shown in Fig. 1(a): the input signal is split into two equal parts by a Y-branch splitter, one of which passes through the upper MMI structure acting as an edge filter 1 while the other passes through the lower MMI structure acting as edge filter 2. A cross section of the SOI rib MMI fabrication technique is shown in Fig. 1(b). The desired spectral responses of the edge filters in the wavelength range from short to long have opposite slopes and are shown in the inset figures of the Fig. 1(c). As shown in Fig. 1(c), the ratios of the two output ports over the desired wavelength range are also presented. Assuming a suitable calibration has been performed in advance, by measuring the ratio of the output powers, the wavelength of an unknown input signal can be measured.

Optics EXPRESS

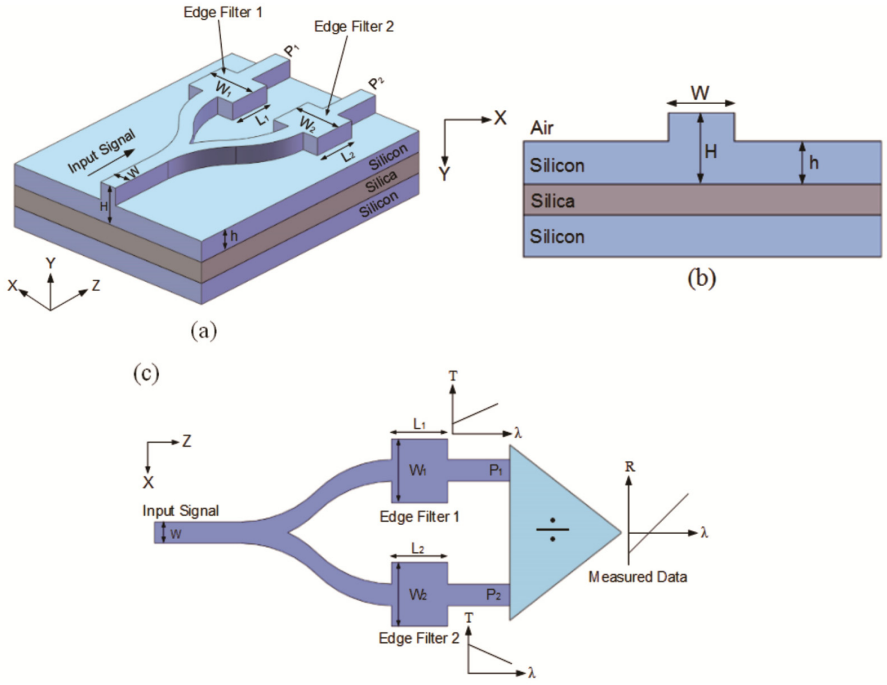

Fig. 1. (a) Schematic configuration of the proposed MMI integrated device; (b) Cross section of SOI rib MMI; (c) Schematic of the proposed MMI ratiometric wavelength monitor.

In the Y-branch splitter, a singlemode input waveguide is split into two singlemode waveguides with a 50:50 power ratio. To design a low-loss broadband Y-branch power splitter, the method described in [16] can be utilized.

Light propagation within the MMI-based devices is often simulated using a modal propagation analysis (MPA) [17]. In the MPA, at the boundary $(z=0)$ between the singlemode waveguide and the multimode waveguide, the input field of the fundamental mode must be the same as the field within the entrance of the multimode waveguide. In other words, at the boundary, the input field can be decomposed into the eigenmodes of the multimode waveguide $\varphi_v(x,y)$. The input field at the entrance of the multimode waveguide can be written as:

$$\psi(x,y,0)=\sum_{v=0}^{m-1}c_v\varphi_v(x,y) \tag{1}$$

where C_v is the excitation coefficient of each mode and m is the number of modes in the multimode waveguide. The coefficient C_v is determined from the overlap integral between $\Psi(x,y,0)$ and $\varphi_v(x,y)$:

$$c_v=\frac{\int\psi(x,y,0)\varphi_v(x,y)dxdy}{\sqrt{\int\varphi_v^{\,2}(x,y)dxdy}} \tag{2}$$

Once the coefficients C_v are obtained, the field at a propagation distance Z within the multimode section can be expressed as:

Optics EXPRESS

$$\psi(x,y,z)=\sum_{\nu=0}^{m-1}c_\nu\varphi_\nu(x,y)\exp\left[j(\beta_\nu-\beta_0)z\right] \tag{3}$$

where β_ν is the propagation constant of each eigenmode of the multimode waveguide. Finally, to obtain the transmissivity (T), the overlap integral between $\psi(x,y,z)$ and the eigenmode of the output singlemode waveguide $\psi_o(x,y)$ is performed. Therefore, the transmissivity in dB can be written as:

$$T(z)=10\cdot\log_{10}\left(\frac{\left|\int\psi(x,y,z)\psi_o(x,y)\,dxdy\right|^2}{\int|\psi(x,y,z)|^2\,dxdy\int|\psi_o(x,y)|^2\,dxdy}\right) \tag{4}$$

It should be noted that $\varphi_\nu(x,y)$ and β_ν can be obtained by using a semi-vectorial finite difference method (FDM) [18].

When using an MMI to implement an edge filter, the MMI width (W) and length (L) are tuned and the transmission response of the MMI is calculated for each W and L. The MPA described above is used to calculate the transmission response in the multimode waveguide. The desired edge filter spectral response corresponds to either an increasing or decreasing transmission response as the wavelength increases over the wavelength range. For a ratiometric wavelength measurement system with a measurable range from λ_1 to λ_2, it is desirable that each edge filter has a low baseline transmission response (T) at either λ_1 or λ_2 and a suitable discrimination of transmission response $D=\left|T(\lambda_1)-T(\lambda_2)\right|$ over the wavelength range [19].

It is well known that a symmetrical MMI has the first self-image distance at $\frac{3}{4}L_\pi$ where L_π is the beat length at a certain wavelength. The self-image distances are repeated for the length of MMI, $L=n\times\frac{3}{4}L_\pi$ with n = 1, 2, 3, and so on. However, at the self-image distances, the MMI has a low wavelength dependence [20], hence it is not suitable for the use as edge filter. To obtain a desired spectral response of the MMI-based edge filter, it is necessary to scan the length of MMI. For example, the MMI length can be scanned from 0 to $2L_\pi$ a which covers the two self-image distances at $\frac{3}{4}L_\pi$ and $2\times\frac{3}{4}L_\pi$.

A parameter scanning method is used by calculating the transmission response over the wavelength range for each W and . It is necessary to calculate the transmission response between the lower and upper limits [λ_1 and λ_2] of the desired wavelength range over a range of W and L values for the MMI. For each of W each MMI, the length L has to be scanned with regular increments to obtain $T(\lambda_1)$ and $T(\lambda_2)$, and thus a corresponding discrimination range D. After this step, suitable structures can be selected by considering their discrimination range D - typically should be D>10 dB and their baseline transmission response - typically less than 10 dB [19].

The spectral response for each of the selected structures is then evaluated. The optimal design for each edge filter should give: i) a baseline transmission response $T(\lambda_2)>-10$ dB

Optics EXPRESS

or $T(\lambda_1) > -10$ dB, for the negative or positive slope, respectively, ii) a discrimination range, $D > -10$ dB, and iii) monotonically increasing or decreasing spectral response.

3. Numerical example

To demonstrate the design method and performance achieved, we present here a numerical example. We choose the refractive indices of the silicon (Si) and silica oxide (SiO_2) used in the SOI MMI rib waveguide of Fig. 1, as 3.4789 and 1.4444 respectively. In order to achieve singlemode operation, the dimensions of the SOI waveguide are optimized [21]. In order to achieve singlemode operation, the dimensions of the SOI waveguide are optimized [21]. A rib singlemode waveguide with H = 5 μm, W = 5 μm, and h = 3 μm, is chosen as input port to adapt the mode profile to that of a singlemode fiber. The edge filter is designed for a wavelength range from λ_1 = 1500 nm to λ_2 = 1600 nm. The width, W, of the MMI is chosen to be in the range 25 – 40 μm. The length, L, of the MMI to be in the range $0 - 2L_\pi(\lambda_1)$ (where $L_\pi = \dfrac{\pi}{\beta_0 - \beta_1}$ and $\beta_{(0,1)}$ is the propagation constant).

The transmission response contours in dB at the two wavelengths 1500 nm and 1600 nm, and the discrimination are presented in Fig. 2. Figure 2(a) and 2(b) show that some values of W and L are associated with a baseline transmission response smaller than −10 dB (white background contour) due to the destructive interferences, hence they are not suited for the use as edge filter. Figure 2(c) shows the values of W and L with the discrimination greater than 10 dB, suitable for the edge filter. For example, an MMI with W = 25 μm and L = $0 - 2L_\pi(\lambda_1)$, it has the transmission responses of −15.02(−11.34) dB for the wavelength of 1500(1600) nm and the discrimination range of 3.68 dB. Thus, it is not suited for the use of edge filter.

By considering the baseline transmission response and the discrimination, the optimal design can be selected. In this case, the optimal edge filters are found to have W_1 = 26 μm, $L_1 = 1.06 \times L_\pi = 2408.6$ μm, and W_2 = 33 μm, $L_2 = 1.17 \times L_\pi = 4173.9$ μm, for the positive slope MMI (T_1) and the negative slope MMI (T_2), respectively. The length, L, of the MMI has to be in the range $0 - 2L_\pi(\lambda_1)$ (where $L_\pi = \dfrac{\pi}{\beta_0 - \beta_1}$ and $\beta_{(0,1)}$ is the propagation constant.

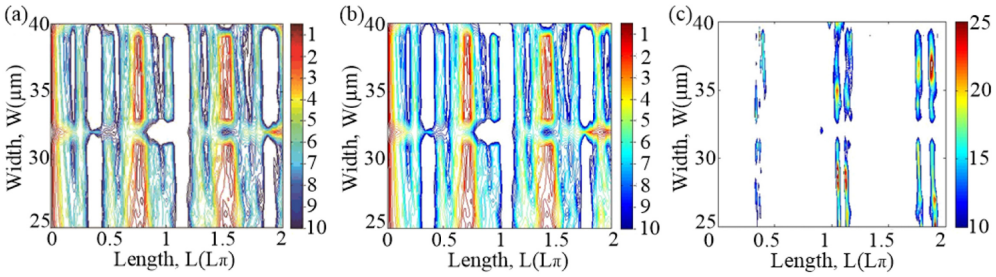

Fig. 2. Contour plots of transmission response (T) in dB under different width and length of MMI (a) at the wavelength λ_1 = 1500 nm, (b) λ_2 = 1600 nm. (c) Discrimination between wavelength λ_2 = 1600 and λ_1 = 1500 nm, $D = |T(\lambda_1) - T(\lambda_2)|$. L_π is set at the wavelength of λ_1.

Optics EXPRESS

The transmission response descibed above was calculated by using the MPA based on FDM. The MPA provides effective computation time for the parameter scanning method to determine the optimal design. For the whole MMI's edge filter structure including input and output waveguide, the optical field distribution in the multimode region of the two MMIs was simulated by using the commercial BPM software (Synopsys Rsoft BeamPro, Pasadena, CA USA) and the results are shown in Fig. 3. Here the length L and the width W of the MMI structures 1 and 2 are L_1 = 2408.6 μm and W_1 = 26 μm, L_2 = 4173.9 μm and W_2 = 33 μm, respectively. All results confirmed that, when the light propagating along the singlemode SOI rib waveguide enters into the multimode SOI rib waveguide section, high-order eigenmodes of the multimode waveguide are excited and interference between different order modes occurs while the light propagates along z direction the multimode SOI waveguide section. Figure 3(a) and 3(b) show that at the wavelength of λ = 1500 nm the output intensity at the output port of MMI1 reaches a maximum, while the intensity of the output port of MMI2 has a minimum. In Fig. 3(c) and 3(d), the output intensity of MMI1 at a wavelength of 1600 nm has a minimum while that of the MMI2 has a maximum, providing the opposite slope response needed.

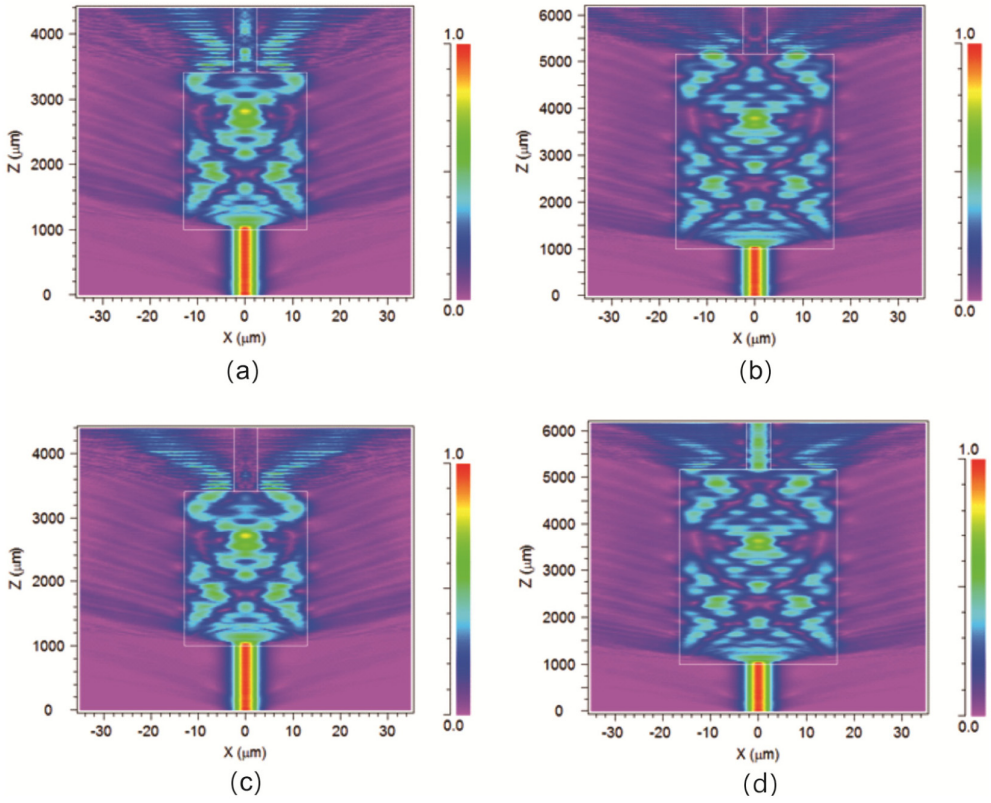

Fig. 3. Distribution of the optical field in the multimode region of the asymmetrical MMIs: (a) MMI1@1500nm; (b) MMI2@1500nm; (c) MMI1@1600nm; and (d) MMI2@1600nm, where MMI1: L_1 = 2408.6 μm, W_1 = 26μm; MMI2: L_2 = 4173.9 μm, W_2 = 33 μm.

The simulated X-type spectral response from the two edge filters is plotted in Fig. 4. For the negative slope edge filter (MMI1), the discrimination range is about 11.55 dB with a baseline loss of −9.04 dB. For the positive slope edge filter (MMI2), the discrimination range (from 1500 nm to 1600 nm) is 12.02 dB, while the baseline loss is −5.93 dB.

Optics EXPRESS

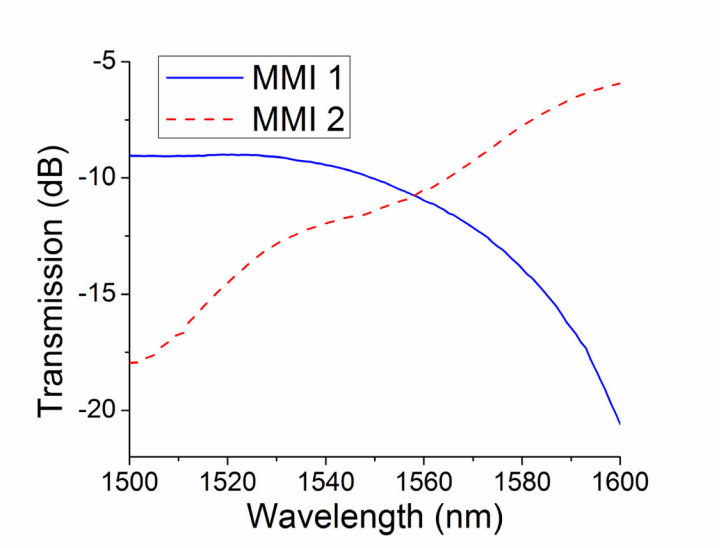

Fig. 4. Calculated transmission spectra of the two MMIs.

4. Device fabrication and ratiometric wavelength measurement

Standard SOI silicon wafers were used as the fabrication medium. Figure 1(b) has clearly shown the basic structure of the device. It comprises a top layer (Si) of thickness 5 μm with a buried layer of thickness 1μm. The fabrication process of the SOI has been optimized for repeatability and ease of future manufacturability with minimal modification. The process comprised six steps: 1) Surface cleaning: the wafer surface was cleaned using acetone, isopropyl alcohol, methanol followed by de-ionized (DI) water, subsequent dehydration was ensured by baking on a hotplate at 120 °C for 3 minutes; 2) Resist fabrication: a PMMA based e-beam resist was deposited on the surface of the cleaned SOI wafer. It was spun at 6000 rpm and prebaked on a hot plate at a temperature of 180 °C for at least 5 minutes which was sufficient to allow complete evaporation of the chlorobenzene solvent as well as sufficient hardening of the resist. This ensured that the PMMA resist layer had the targeted thickness of about 300 nm; 3) Photolithography: a JEOL JBX-9300FS Electron Beam Lithography (EBL) system with 20 nm resolution and accelerating voltage of 10 kV was used for this purpose; the electron dose was optimized to ensure the resulting patterned waveguide was equivalent to the targeted sizes; 4) Photoresist Development: a 3:1 mixture of methyl isobutyl ketone (MIBK) and isopropyl alcohol (IPA) was applied for 20 seconds and subsequently rinsed in IPA for 25 seconds; 5) Dry etching: inductively coupled plasma (ICP) etching using an ICP-RIE process (Plasmalab System 100, Oxford Instruments) was applied in conjunction with fluoride gas. The etch rate was about 200 nm/min, sufficient for effective and rapid manufacture of the device. Here minimum sidewall roughness is an essential feature of the fabricated device and the etching phase has been optimized to ensure this condition is met; 6) Photoresist removal and final device preparation: the photoresist was removed using O_2 plasma, and then the fabricated integrated devices were subsequently cleaned and cut from the wafer. Final polishing on both sides of the wafer was undertaken for device optical characterization and ratiometric measurement. Figure 5(a) shows an SEM image of an SOI MMI arm. Figure 5(b) shows the integrated device consisting of both the two SOI MMIs.

Optics EXPRESS

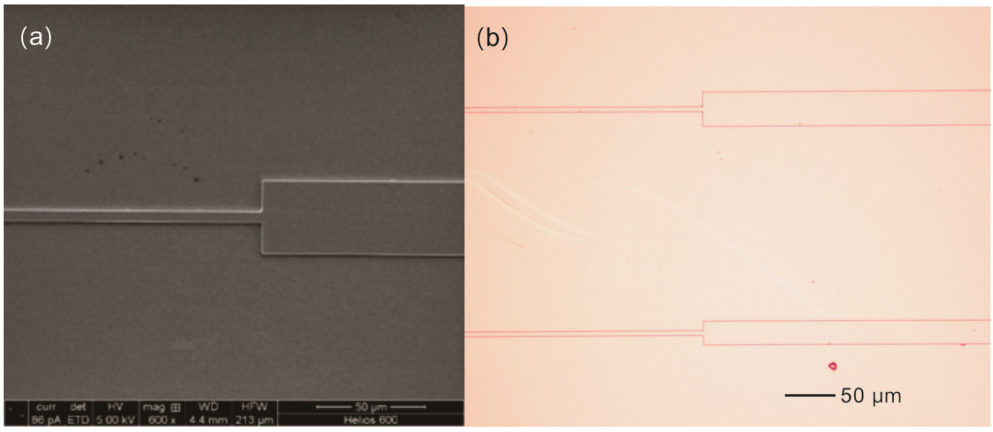

Fig. 5. (a) SEM image of one of the MMI arms with a width of 33 µm; (b) SEM snapshot of the two symmetrical SOI MMIs used for the proposed ratiometric wavelength monitoring.

The ratiometric transmission spectrum was measured by using a tunable laser source which was coupled to the SOI integrated device using singlemode fibers connecting a polarization controller and a tapered singlemode fiber. In order to collect the output signal, two 20X objective lenses and two photodiodes were placed at the end of each SOI output ports, the optical power was collected separately and hence the power ratio was calculated and processed by the integrated wavelength monitoring system. Figure 6 shows the measured and simulated ratio results: the measured data has a good agreement with the calculated results, although measured results of the SOI photonic integrated device are smaller than those predicted by calculations. The observed worst case of 25.2% discrepancy between the simulated and measured results is shown in Fig. 6, thus pointing to a number of possible reasons, such as the imprecise refractive indices used in the theoretical models, or more likely, the slab thickness of the SOI (both singlemode and multimode SOI waveguides) and physical dimensions deviations of the MMI waveguides during the fabrication, namely the manufacturing tolerances.

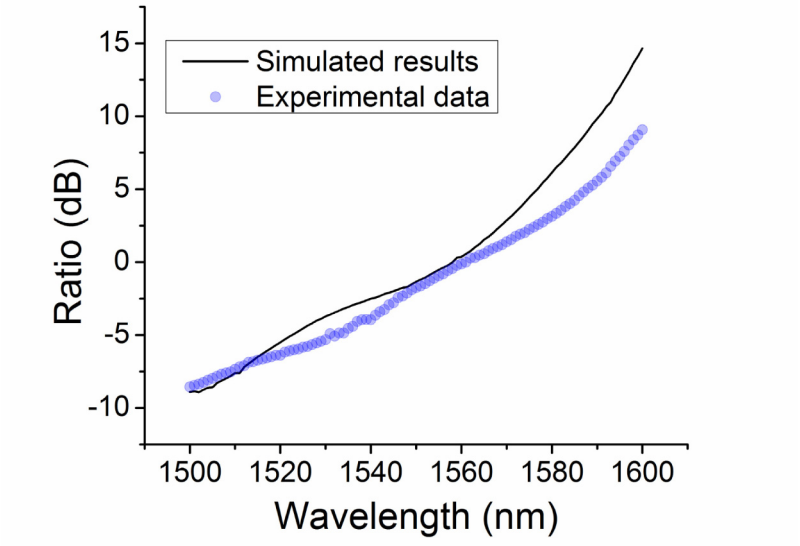

Fig. 6. Simulated and measured ratio results.

Optics EXPRESS

To evaluate the wavelength discrimination ability and also the wavelength resolution of the proposed photonic integrated SOI MMI device, the ratiometric wavelength measurement process was performed using the experimental method presented in [22, 23], considering the optical and the electrical noise of the source signal and of the photodetectors. In the experiments, the SNR of the input tunable lasing signal generated by a narrow linewidth, high precision tunable laser (Agilent 81600B, Santa Clara, CA USA), is better than 70 dB, while the resolution of the high sensitive power meters (ADC 8250A, Tokyo Japan) is 0.001 dB and the noise generated by the power meters and electronic circuitry is equivalent to an reproducibility error in the ratiometric measurements of about 0.002 dB. The starting source wavelength was set to λ = 1550 nm and then the wavelengths were shifted by increasing increments of 10, 15, 20, and 25 pm, successively. The power meter outputs were sampled every 10 seconds and the ratio of the power meter outputs was measured for each wavelength.

Figure 7 shows the measured ratio values within the complete time series as a function of sample time starting from λ = 1550 nm. The wavelength was stepped by successively increasing increments of 10, 15, 20, and 25 pm every 10 seconds. The figure shows the clearly detectable change of the recorded output ratio of the proposed passive wavelength monitoring system, capable of achieving a resolution of better than 15 pm, which is competitive compared with some commercial active wavelength scanning techniques and has the additional advantages of robustness and the absence of a need for mechanical movement. The other wavelengths of 1500 and 1600 nm provide a resolution better than 20 and 10 pm. Also compared with our previous work on optical fiber based edge filters [3, 19, 23], the advantage of this work is that silicon photonics is an unique candidate that should be qualified for integrating both electronics and photonics on the same optoelectronic circuit chip, leading to a high-volume production of low-cost devices on silicon platform by using the standard photolithography technologies from the microelectronics industry. Ref [8] demonstrated that the wavelength measurement based on Fano resonance in microring resonator can have a high resolution of 0.8 pm but with a short wavelength range of 0.47 nm. Also, the next generation of photonic components needs to meet ease of fabrication, compact physical configuration, low-cost, CMOS compatibility, broadband operation (especially challenging at the mid-infrared wavelength range) and compatible with high-volume manufacturing. Silicon photonics appears as a unique platform to deal with this integration challenge using highly confined optical modes in silicon based photonic integrated circuits.

Optics EXPRESS

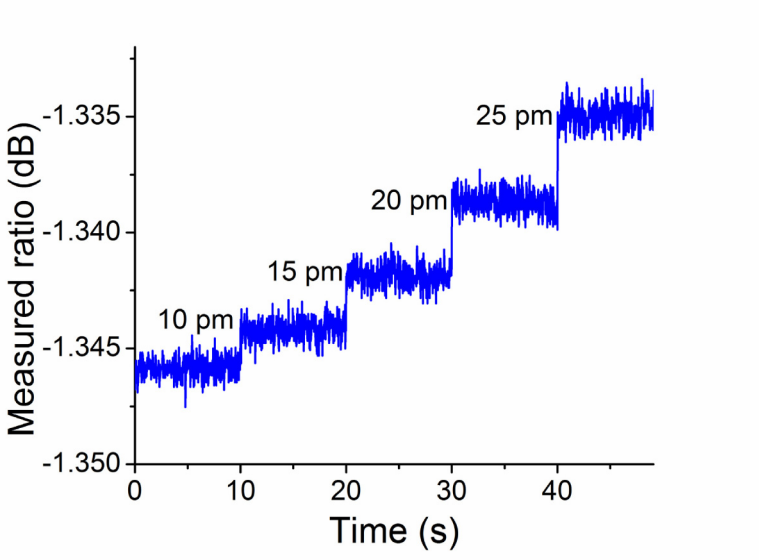

Fig. 7. Output ratio as the wavelength is tuned from a start wavelength of 1550 nm.

5. Conclusion

In conclusion, an integrated SOI device based on a pair of symmetrical MMI structures with X-type spectral response for wavelength monitoring has been investigated theoretically and experimentally. The wavelength discrimination of the proposed ratiometric structure has been investigated and has shown a competitive measurement resolution better than 15 pm for a wavelength monitoring application with a range of advantages, such as a simpler configuration and a low-cost as compared to existing ratiometric wavelength monitoring systems. Furthermore, the proposed SOI asymmetric MMIs integrated device shows promising characteristics, making them potentially suitable for on-chip wavelength monitoring of large scale Si-PICs. Future work will focus on the post-processing techniques for improving the performance of the integrated device, such as annealing and device packaging process.

Funding

111 project (B13015) at the Harbin Engineering University; Key Program for International S&T Cooperation Projects of China under grant 2016YFE0126500; National Natural Science Foundation of China (NSFC) under grant 61575050; Key Program for Natural Science Foundation of Heilongjiang Province of China under grant ZD2016012; Science Foundation Ireland (SFI) under the National Access Programme 179; SFI under the International Strategic Cooperation Award Grant Number SFI/13/ISCA/2845; the Royal Society (London).

Acknowledgment

We thank Mr. Neil Sessions for his help with the experiments.